Elevated surface chlorophyll associated with natural oil seeps in the Gulf of Mexico

D'souza N.A.[1,3]; Subramaniam A.[1]; Juhl A.R.[1]; Hafez M.[1]; Chekalyuk A.[1]; Phan S.[1]; Yan B.[1]; MacDonald I.R.[2]; Weber S.C.[3]; Montoya J.P.[3]

[1] Lamont-Doherty Earth Observatory of Columbia University, Palisades, NY

[2] Florida State University, Tallahassee, Florida

[3] Georgia Institute of Technology, Atlanta, Georgia.

Natural hydrocarbon seeps occur on the seafloor along continental margins, and account for up to 47% of the oil released into the oceans[1]. Hydrocarbon seeps are known to support local benthic productivity[2], but little is known about their impact on photosynthetic organisms in the overlying water column. Here we present high temporal and spatial resolution observations of chlorophyll concentrations in the Northern Gulf of Mexico using *in-situ* and shipboard flow-through fluorescence measurements from May to July 2012, as well as an analysis of ocean-colour satellite images from 1997 to 2007. All three methods reveal elevated chlorophyll concentration in waters influenced by natural hydrocarbon seeps found at depths greater than 1000m. Temperature and nutrient profiles above seep sites suggest that nutrient-rich water upwells from depth, facilitating phytoplankton growth and thus supporting the higher chlorophyll concentrations observed. Since upwelling occurs at natural seep locations around the world[1, 2, 3], we conclude that offshore hydrocarbon seeps, and perhaps other types of deep ocean vents and seeps, may influence biogeochemistry and productivity of the overlying water column.

Natural hydrocarbon seeps occur on the seafloor along continental margins, where gaseous and liquid hydrocarbons migrate from deep reservoirs into unconsolidated sediments near the seafloor and some of this fluid is released through focused vents[4, 5]. In the Gulf of

Mexico, such seeps frequently emit plumes of oil and gas into the water column, releasing up to 1.1×10^8 L oil yr^{-1} (6). A significant percentage of the released hydrocarbons are consumed and mixed along their ascent through the water column from depths that can exceed 2000 m (5). Although rising hydrocarbon plumes can be advected laterally by sub-surface currents, in the Gulf of Mexico, they typically surface within a ~3-km radius of their seafloor origin[7]. Wind and surface currents then shape the resulting ~0.1-µm thick oil-slicks into patches up to several hundred meters wide and kilometers long[5, 7] that can then be detected by satellite remote sensing. These slicks gradually dissipate through spreading, flocculation, dissolution, evaporation and weathering over subsequent days[8].

MacDonald et al.[9] used Synthetic Aperture RADAR imagery of surface oil-slick features to map the locations of putative natural oil seeps in the Northern Gulf of Mexico. Using a combination of ROV dives and satellite remote sensing, they found that even the most prolific sites exhibited some episodicity in the seepage of oil and gas. Some of the most persistent slicks were associated with the Green Canyon reservoir (GC), and the site denoted as GC600 is one of the best-studied natural hydrocarbon seep sites in the Gulf of Mexico[10], located at a depth of approximately 1200 m.

GC600 and other sites away from seeps were studied during a shipboard survey in the Northern Gulf of Mexico in May-July 2012 (Supplementary Table 1). Vertical profiles of the water column made with a Conductivity-Temperature-Depth (CTD) rosette system with a chlorophyll fluorometer showed that chlorophyll concentrations at the deep chlorophyll maximum near GC600 were significantly elevated compared to non-seep, background sites (Wilcoxon Rank Sum Test, $P = 0.01$; Fig. 1a), with mean chlorophyll concentration at the seep chlorophyll maximum (0.66 ± 0.03 mg m^{-3}) more than double that of background sites (0.29 ±

0.02 mg m^{-3}). The depth of the average chlorophyll maximum was shallower at seep sites (82m) compared to the background sites (99m). Depth-integrated chlorophyll concentrations at GC600 were also significantly higher than the background sites (Wilcoxon Rank Sum Test, $P = 0.01$), with integrated chlorophyll at the seep averaging 28.2 ± 1.1 mg m^{-2} vs. 22.3 ± 1.8 mg m^{-2} for background sites. The increase in chlorophyll may be attributable to elevated nutrient concentrations between 50-200 m at GC600 relative to non-seep sites (Fig. 1b, Supplementary Table 2). A possible explanation for the elevated nutrient concentrations is indicated in temperature profiles showing colder water at GC600 between 50 m and about 1000 m compared to background sites (Fig. 1c, Supplementary Fig. 1), suggesting the upwelling of colder, nutrient-rich waters at GC600.

Turbulence generated by buoyant bubble plumes originating at natural seeps can draw surrounding water into the rising bubble stream to generate upwelling flows that persist at least up to the pycnocline. These strong episodic upwelling flows manifest as colder water compared to background in hydrographic profiles of the water column above seep locations and have been observed at both shallow[11] and deep[12] seeps. Plume-generated upwelling above seeps could exert a "bottom-up" influence on near-surface microbes similar to eddy-driven upwelling that has been shown to episodically supply nutrients to phytoplankton in subtropical waters[13]. The transport of bubbles from depths greater than 1000 m has been observed in echo-sounder data in the Gulf of Mexico[5, 6], in the Norwegian-Barents-Spitzbergen continental margin[12], and the Black Sea[14] and likely happens at hydrocarbon seeps elsewhere in the world.

Elevations in localized chlorophyll concentration were not restricted to the deep chlorophyll maximum layer, though near-surface increases in chlorophyll above seep sites were more subtle and exemplified the intermittent nature of the driving mechanisms. During three oceanographic cruises, high temporal and spatial resolution chlorophyll fluorescence data were acquired using an Aquatic Laser Fluorescence Analyzer (WETLabs)[15] plumbed to the ship's flow-through system to continuously measure chlorophyll concentrations in near-surface waters along the ship track. Observations along ship tracks near GC600 were separated into "seep" and "non-seep background" categories based on proximity (> or < 3 km) to the seafloor coordinates of GC600 (Fig. 2). To exclude the Mississippi River plume, comparisons between categories were only made for sections of the ship track near GC600 with salinities > 35.6. While there was a slight decrease in surface chlorophyll concentrations at GC600 compared to background during the May-July 2012 cruise (consistent with the vertical profiles in Fig. 1a), during the other two cruises (in September 2012 and June 2013) near-surface chlorophyll concentrations at GC600 were significantly elevated relative to corresponding background areas nearby (Wilcoxon Rank Sum test, $P < 0.001$ for each comparison, Fig. 2b, c, Supplementary Table 3). Moreover, the range and variance of near-surface chlorophyll concentrations were higher in all three visits to the GC600 site compared to nearby background. Maximum near-surface chlorophyll concentrations at GC600 were remarkably higher than corresponding background values, with an average elevation > 300%. Episodic upwelling could explain both the higher chlorophyll maxima and variance near the seep. Moreover, chlorophyll concentrations at these sites were skewed towards the higher end of the distribution, with higher kurtosis values suggesting that the increase in variance was related to infrequent extreme values, rather than multiple modest increases.

The coincidence between near-surface oil inputs and chlorophyll enhancement is best demonstrated on larger scales by comparing satellite observations of surface oil slicks with satellite-derived chlorophyll concentrations. The database of putative natural oil seeps was remapped onto 10 x 10 km grids to identify the single grid cell with the highest cumulative surface area covered by slicks between 1997 to 2007 (site Alpha). Four locations that had no observed oil slicks were also identified to provide non-seep, background conditions for comparison. The 8-day, 9-km average satellite-derived chlorophyll concentration [chl_8] within 50 x 50 km boxes (the red and black boxes in Fig. 3a, based on two grid cells in each direction from the central cell) was extracted for each of the 5 locations centered on Alpha and the 4 background sites to generate time series. Between 1997 - 2007, [chl_8] could be calculated before and after the observation of 23 oil slicks directly inside the 10 x 10 km Alpha box. For these observed 23 slick events, the change in 8-day chlorophyll concentration Δ[chl_8] around Alpha for the time interval that followed the slick was significantly greater than concurrent changes averaged across the four non-seep background locations during the same 8-day period (Fig. 3b, c; Wilcoxon Signed-Rank test, $P = 0.01$). This suggests that changes in chlorophyll concentrations observed at Alpha following slicks were not caused by broad regional environmental factors, common with the background sites. In contrast, if slick events observed at site Alpha were excluded from the time series, values of Δ[chl_8] at Alpha were not significantly different from the corresponding mean background values (Wilcoxon Signed-Rank test, $P = 0.22$). Thus, Δ[chl_8] at Alpha only deviated significantly from background for the time periods following observation of a surface slick at Alpha.

The SAR image database for this region was discontinuous (with only 176 distinct acquisitions over the 10 year study period). Combining infrequent imaging with the sporadic nature of seepage and cloud cover (that obscures satellite-derived chlorophyll), and the necessity for calm surface conditions for slick detection using SAR imagery suggests that the influence of natural seeps on chlorophyll concentrations was almost certainly underestimated by the satellite observations. Nevertheless, the satellite observations uniquely link the increases in chlorophyll concentrations at Alpha to the episodic transport of oil and other material from the deep sea to the surface ocean, potentially connecting episodic upwelling of nutrients to the supply of hydrocarbons.

The connection between elevated chlorophyll and oil at seep sites may be more complex than the nutrient upwelling scenario presented initially. Oil reaching the upper water column impacts an intricately interconnected microbial community including oil-degrading bacteria, cyanobacteria, eukaryotic phytoplankton, protistan grazers, and viruses[16]. Interactions among these organisms and their environment can result in negative or positive feedbacks on phytoplankton biomass. Hydrocarbon degradation by heterotrophic bacteria in near-surface waters can be rapid, but is typically nutrient limited[16, 17] and these bacteria may outcompete phytoplankton for the available nutrients. Fresh crude oil is toxic to phytoplankton at high concentrations[18, 19], but can have either inhibiting or stimulating effects at low concentrations depending on the species composition of the phytoplankton assemblage[20], the influence of protistan grazers[16, 21, 22], nutrient concentrations[16, 23], the type of oil[24], and the duration of exposure[25]. Protistan grazers, which may be fairly tolerant of crude oil contamination[22, 26], play an important ecological role in aquatic microbial communities, both as consumers of bacteria and phytoplankton, and in the recycling of limiting nutrients[22]. Increases in phytoplankton biomass following oil spills have been attributed to an indirect “top down” effect through predation on bacteria that compete with phytoplankton for nutrients[27, 28]. Thus, the episodic influx of nutrients and hydrocarbons into the upper water column at seep sites could affect local phytoplankton abundance through direct, “bottom-up” effects on phytoplankton growth rate, or through indirect “top-down” effects mediated through the planktonic food web. These nutrient and grazing hypotheses explaining increased chlorophyll at seep sites should not be thought of as mutually exclusive[29] and need further study, with sufficient spatial and temporal resolution to resolve the underlying processes in light of the high variability we have documented.

Three independent observation methods – vertical profiles and near-surface *in-situ* fluorometry, as well as broad-scale remote sensing – revealed localized increases in phytoplankton biomass above natural hydrocarbon seeps that in aggregate have regional implications for productivity, carbon and nutrient cycling, and food-web dynamics in the ecologically and economically important Northern Gulf of Mexico. These observations have afforded an unprecedented view into a highly variable and previously undescribed process that connects sea-floor features at depths exceeding 1000 m to biological processes in the overlying euphotic zone. Given the global abundance and distribution of offshore hydrocarbon seeps[1] , these observations in the Gulf of Mexico likely reflect a world-wide phenomenon. They also raise the possibility that other types of deep ocean vents and seeps may have subtle influences in their overlying water column, influences that would likely only be detected with purposeful high temporal and spatial resolution sampling.

References:

1. Judd AG. The global importance and context of methane escape from the seabed. *Geo-Mar Lett* 2003, **23**(3-4)**:** 147-154.

2. Hovland M, Jensen S, Fichler C. Methane and minor oil macro-seep systems — Their complexity and environmental significance. *Mar Geol* 2012, **332-334:** 163-173.

3. Milkov AV. Global gas flux from mud volcanoes: A significant source of fossil methane in the atmosphere and the ocean. *Geophys Res Lett* 2003, **30**(2).

4. Roberts HH, Carney RS. Evidence of episodic fluid, gas, and sediment venting on the northern Gulf of Mexico continental slope. *Econ Geol* 1997, **92**(7-8)**:** 863-879.

5. MacDonald IR, Leifer I, Sassen R, Stine P, Mitchell R, Guinasso N. Transfer of hydrocarbons from natural seeps to the water column and atmosphere. *Geofluids* 2002, **2**(2)**:** 95-107.

6. Solomon EA, Kastner M, MacDonald IR, Leifer I. Considerable methane fluxes to the atmosphere from hydrocarbon seeps in the Gulf of Mexico. *Nat Geosci* 2009, **2**(8)**:** 561-565.

7. Garcia-Pineda O, MacDonald I, Zimmer B, Shedd B, Roberts H. Remote-sensing evaluation of geophysical anomaly sites in the outer continental slope, northern Gulf of Mexico. *Deep Sea Res Part II* 2010, **57**(21-23)**:** 1859-1869.

8. Macdonald IR, Guinasso NL, Ackleson SG, Amos JF, Duckworth R, Sassen R, *et al.* Natural oil-slicks in the gulf-of-mexico visible from space. *J Geophys Res* 1993, **98**(C9)**:** 16351-16364.

9. MacDonald IR, Garcia-Pineda O, Beet A, Asl SD, Feng L, Graettinger G*, et al.* Natural and Unnatural Oil Slicks in the Gulf of Mexico. *J Geophys Res* Accepted.

10. Roberts HH, Feng D, Joye SB. Cold-seep carbonates of the middle and lower continental slope, northern Gulf of Mexico. *Deep Sea Res Part II* 2010, **57**(21-23)**:** 2040-2054.

11. Leifer I, Jeuthe H, Gjøsund SH, Johansen V. Engineered and Natural Marine Seep, Bubble-Driven Buoyancy Flows. *J Phys Oceanogr* 2009, **39**(12)**:** 3071-3090.

12. Sauter EJ, Muyakshin SI, Charlou J-L, Schlüter M, Boetius A, Jerosch K*, et al.* Methane discharge from a deep-sea submarine mud volcano into the upper water column by gas hydrate-coated methane bubbles. *Earth Planet Sci Lett* 2006, **243**(3-4)**:** 354-365.

13. McGillicuddy DJ, Jr., Anderson LA, Bates NR, Bibby T, Buesseler KO, Carlson CA*, et al.* Eddy/wind interactions stimulate extraordinary mid-ocean plankton blooms. *Science* 2007, **316**(5827)**:** 1021-1026.

14. Körber J-H, Sahling H, Pape T, dos Santos Ferreira C, MacDonald I, Bohrmann G. Natural oil seepage at Kobuleti Ridge, eastern Black Sea. *Mar Pet Geol* 2014, **50:** 68-82.

15. Chekalyuk A, Barnard A, Quigg A, Hafez M, Zhao Y. Aquatic laser fluorescence analyzer: field evaluation in the northern Gulf of Mexico. *Optics Express* 2014, **22**(18)**:** 21641-21656.

16. Head IM, Jones DM, Roling WF. Marine microorganisms make a meal of oil. *Nat Rev Microbiol* 2006, **4**(3)**:** 173-182.

17. Atlas RM. Microbial degradation of petroleum hydrocarbons: An environment perspective. *Microbial Reviews* 1981, **45:** 180-209.

18. Dunstan W, Atkinson L, Natoli J. Stimulation and inhibition of phytoplankton growth by low molecular weight hydrocarbons. *Mar Biol* 1975, **31**(4)**:** 305-310.

19. Huang YJ, Jiang ZB, Zeng JN, Chen QZ, Zhao YQ, Liao YB*, et al.* The chronic effects of oil pollution on marine phytoplankton in a subtropical bay, China. *Environ Monit Assess* 2011, **176**(1-4)**:** 517-530.

20. Prouse NJ, Gordon Jr DC, Keizer PD. Effects of low concentrations of oil accommodated in sea water on the growth of unialgal marine phytoplankton cultures. *Journal of the Fisheries Board of Canada* 1976, **33**(4)**:** 810-818.

21. Dalby AP, Kormas KA, Christaki U, Karayanni H. Cosmopolitan heterotrophic microeukaryotes are active bacterial grazers in experimental oil-polluted systems. *Environ Microbiol* 2008, **10**(1)**:** 47-56.

22. Stoeck T, Edgcomb V. Role of Protists in Microbial Interactions with Hydrocarbons. In: Timmis KN (ed). *Handbook of Hydrocarbon and Lipid Microbiology*. Springer-Verlag Berlin: Heidelberg, 2010, pp 2423-2434.

23. Atlas RM. Microbial degradation of petroleum hydrocarbons: an environmental perspective. *Microbiol Rev* 1981, **45**(1)**:** 180-209.

24. Bate G, Crafford SD. Inhibition of phytoplankton photosynthesis by the WSF of used lubricating oil. *Mar Pollut Bull* 1985, **16**(10)**:** 401-404.

25. Vargo G, Hutchins M, Almquist G. The effect of low, chronic levels of No. 2 fuel oil on natural phytoplankton assemblages in microcosms: 1. Species composition and seasonal succession. *Marine Environmental Research* 1982, **6**(4)**:** 245-264.

26. Rogerson A, Berger J. Effect of crude oil and petroleum-degrading micro-organisms on the growth of freshwater and soil protozoa. *Journal of General Microbiology* 1981, **124**(1)**:** 53-59.

27. Teal JM, Howarth RW. Oil-Spill Studies - a Review of Ecological Effects. *Environmental Management* 1984, **8**(1)**:** 27-43.

28. Fleeger JW, Carman KR, Nisbet RM. Indirect effects of contaminants in aquatic ecosystems. *Sci Tot Environ* 2003, **317**(1-3)**:** 207-233.

29. Juhl AR, Murrell MC. Interactions between nutrients, phytoplankton growth, and microzooplankton grazing in a Gulf of Mexico estuary. *Aquatic Microbial Ecology* 2005, **38**(2)**:** 147-156.

Supplementary Information is linked to the online version of the paper at www.nature.com/nature

Author Information: Correspondence and requests for materials should be addressed to ndsouza@ldeo.columbia.edu or ajit@ldeo.columbia.edu.

Acknowledgements:

We thank the science parties and ship's crew of the *R/V Endeavor* for their assistance with multiple shipboard operations. We thank Oscar Garcia-Pineda for his assistance in providing the TCNNA derived database of putative natural oil seeps. We thank Katelyn Geddes for assistance with chlorophyll extractions used in ALFA calibrations. This work is supported by The Gulf of

Mexico Research Initiative's (GOMRI) ECOGIG consortium, with additional support from NSF grant NSF-OCE-0928495 to J.M. and NASA grant NNX10AT99G to A.S. This is LDEO contribution number 7951, and ECOGIG contribution number 365. Data are available from the Gulf of Mexico Research Initiative Information and Data Cooperative (http://data.gulfresearchinitiative.org: R1.x132.134:0003, R1.x132.134:0005, R1.x132.139:0025).

Author contributions: A.S., A.J., B.Y., J.M., and N.D. designed the study. M.H, A.C., and S.P. helped analyze the data. N.D., A.J., and A.S. wrote the paper. I.M. collected and processed SAR images to produce databases of oil slicks and putative seep locations across the Gulf of Mexico. A.S. and S.P. collected and processed satellite images and data for analysis of chlorophyll concentrations associated with slick events. N.D., M.H., and A.C. collected and processed data for the shipboard *in-situ* fluorometry. N.D., M.H., A.J., S.W., and J.M. deployed the CTD and analyzed the data. S.W. and J.M. collected and processed nutrients samples. All authors discussed the results and commented on the manuscript.

The authors declare no competing financial interests.

Figure Legends:

Figure 1: Water column profiles of chlorophyll, nutrients, and temperature above seep GC600 and background sites. Average seep (red) and non-seep background (blue) chlorophyll concentrations (**a**), nitrate plus nitrite concentrations (**b**), and temperatures (**c**) from multiple

CTD casts at GC600 and non-seep sites. Panels **a** and **c** derive from 9 seep and 10 non-seep CTD casts. Data are means ±1 s.e.m for 1-m depth bins. In **b** data are means ±1 s.e.m for both depth and concentration. Supplementary Table 2 has further details on nutrient data. Dotted horizontal lines show the mean depths of seep (red) and non-seep (blue) deep chlorophyll maxima.

Figure 2: Transects of near-surface chlorophyll concentrations near seep GC600. Surface chlorophyll concentrations were measured near GC600 during three cruises using shipboard flow-through fluorometry. Observations along ship tracks were separated into "seep" (90.6°W – 90.53°W) and "non-seep background" (90.53°W - 90.1°W) categories based on distance from GC600. The plots show chlorophyll concentration at each location with color of the dots indicating salinity according to the right-hand legend. Transects were truncated where salinity dropped below 35.6.

Figure 3: Changes satellite derived chlorophyll concentrations following oil slick events. (**a)**, Map showing the 10 × 10 km grid cells used to quantify oil slicks and the 50 x 50 km boxes surrounding site Alpha (red), and the four background sites (black) used to quantify chlorophyll concentration. . (**b)**, changes in chlorophyll concentration in the 50 × 50 km area around Alpha (black) and background sites (gray) from one 8-day interval to the next (Δ[chl$_8$]) when a slick was observed at Alpha. The median Δ[chl$_8$] at Alpha and background sites across all slick events are shown by the red and blue dotted lines.

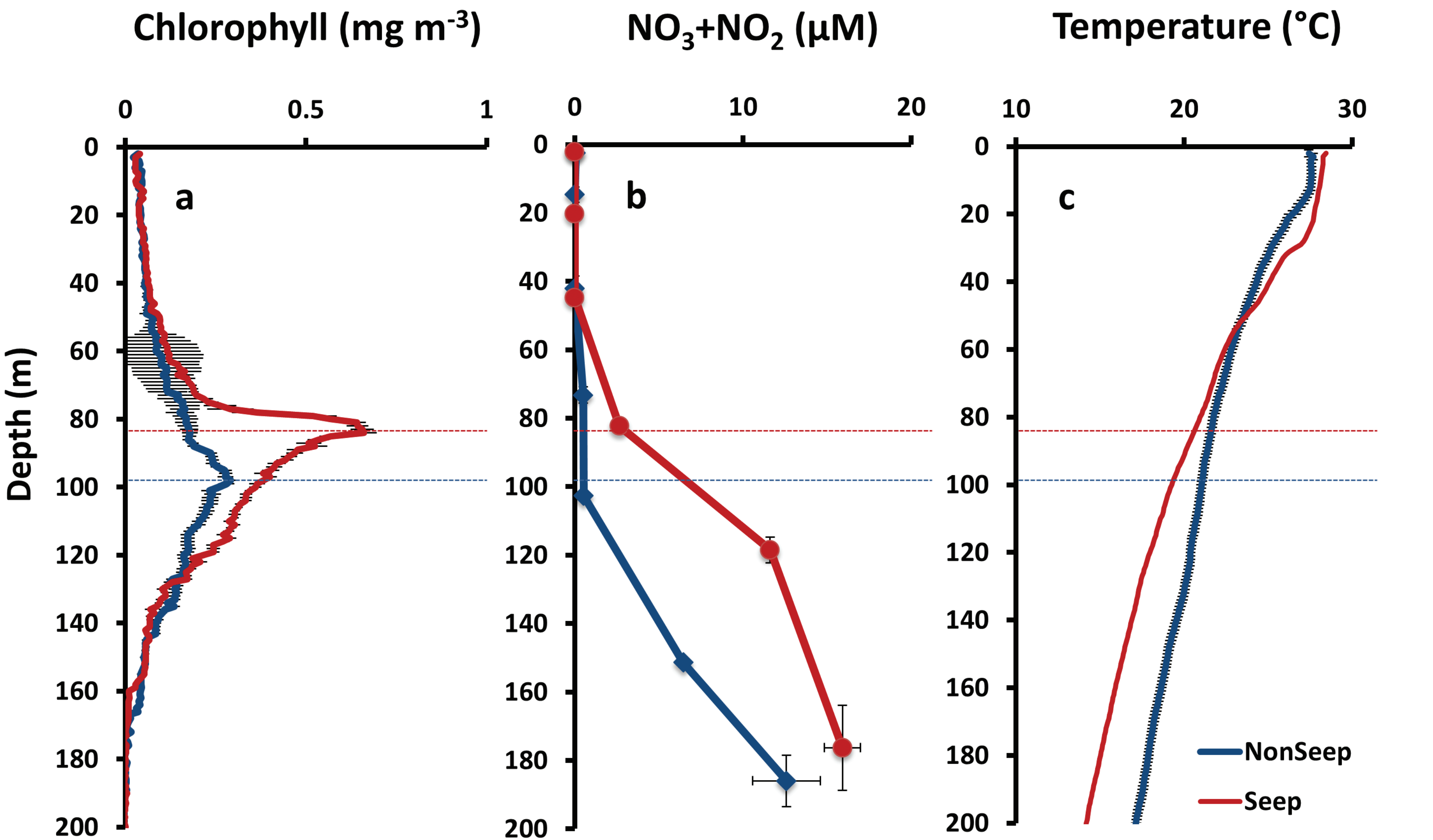

Chlorophyll (mg m-3)
NO3+NO2 (µM)
Temperature (°C)
0
0.5
1
0
10
20
10
20
30
Depth (m)
0
20
40
60
80
100
120
140
160
180
200
a
b
c
NonSeep
Seep

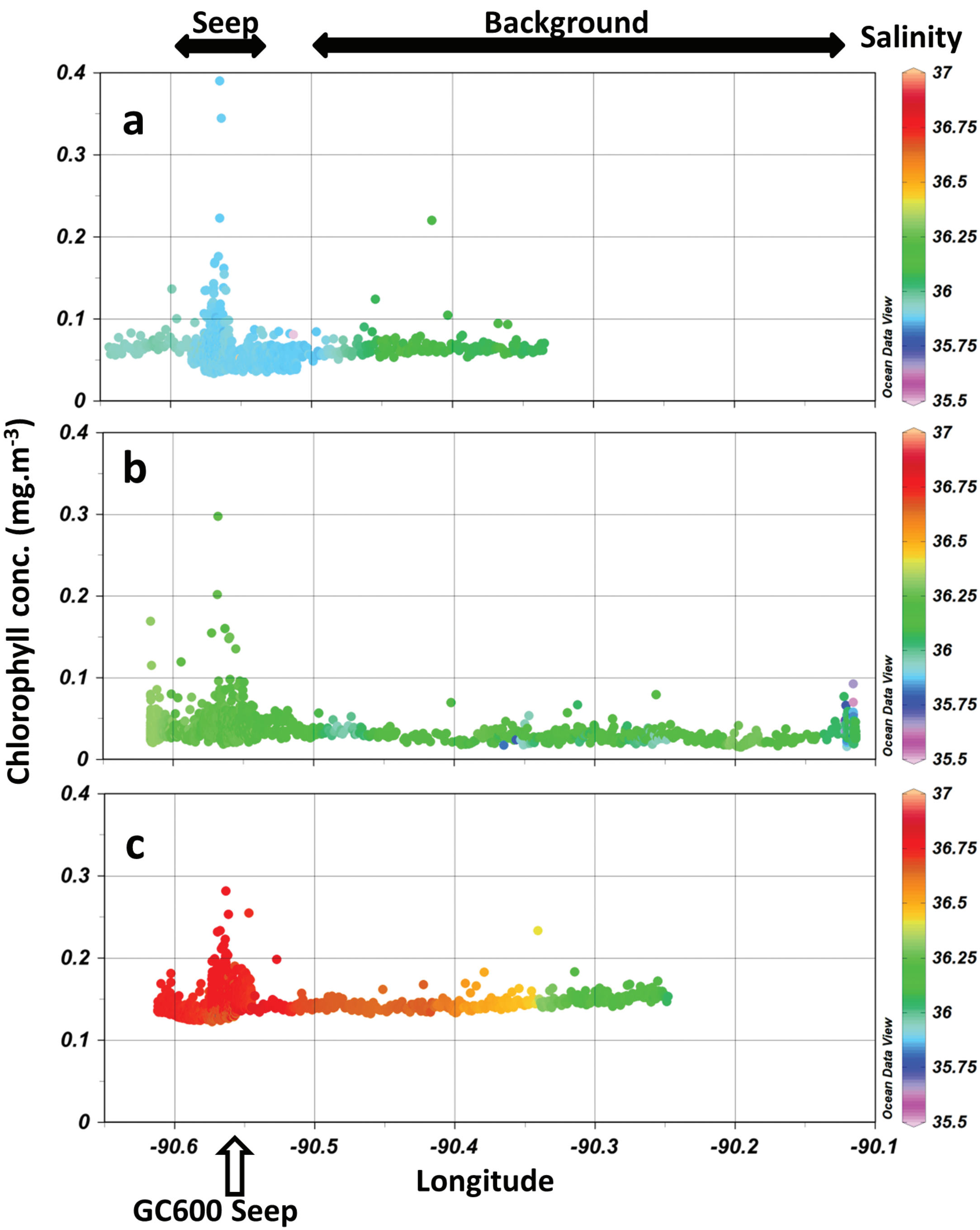

Seep
Background
Salinity
a
b
c
Chlorophyll conc. (mg.m-3)
0.4
0.3
0.2
0.1
0
37
36.75
36.5
36.25
36
35.75
35.5
Ocean Data View
-90.6
-90.5
-90.4
-90.3
-90.2
-90.1
Longitude
GC600 Seep

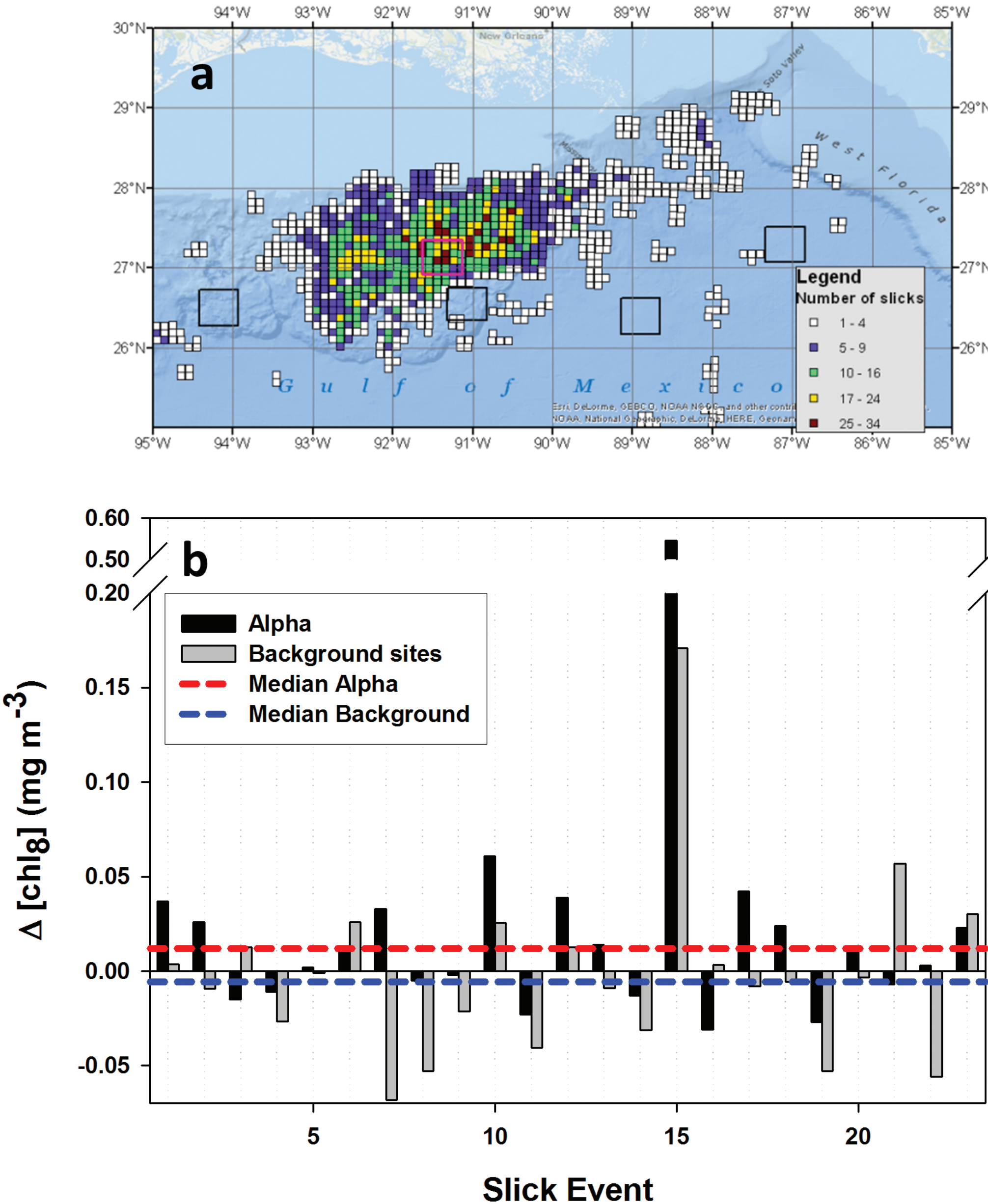

a
94°W 93°W 92°W 91°W 90°W 89°W 88°W 87°W 86°W 85°W
30°N
29°N
28°N
27°N
26°N
95°W
New Orleans
Soto Valley
West Florida
Gulf of Mexico
Legend
Number of slicks
1 - 4
5 - 9
10 - 16
17 - 24
25 - 34
b
0.60
0.50
0.20
0.15
0.10
0.05
0.00
-0.05
Alpha
Background sites
Median Alpha
Median Background
Δ [chl8] (mg m-3)
5
10
15
20
Slick Event

Methods:

Hydrography:

GC600 and comparable non-seep locations in the northern Gulf of Mexico were sampled during a cruise on board the *R/V Endeavor* in May-July 2012. Nine water column profiles were made at GC600 and 10 profiles were made at the non-seep background stations (Supplementary Table 1) using a water-sampling rosette equipped with a Seabird 11+ CTD and a Wetlabs ECO-AFL chlorophyll fluorometer. Nutrient samples ($NO_3^- + NO_2^-$, PO_4^{3-}, SiO_2) were collected from Niskin bottles fired at slightly different depths on each CTD cast and analyzed at sea within six hours of collection using a Lachat QuikChem 8000 flow-injection analysis system (Lachat Instruments, Loveland CO, USA)[1]. For comparison between seep and background categories, chlorophyll concentrations, nutrient concentrations, and temperature from each CTD cast were first averaged into depth bins (1-m bins for chlorophyll and temperature, variable depth bins for nutrients, see Supplementary Table 2) and then combined to calculate average seep and background profiles.

Along-track fluorometry:

An Aquatic Laser Fluorescence Analyzer (ALFA, WETLabs)[2] was used to measure laser-induced fluorescence emission spectra in near-surface waters during three cruises that passed over GC600 on the *R/V Endeavor* (June-July 2012, September 2012, and June-July 2013). The ALFA was connected to the ship's underway intake, receiving water pumped from approximately 5 m depth at a flow rate of 2.2 L/min. Using 405 and 514 nm excitation lasers, the ALFA acquired two fluorescence emission spectra between 400 to 800 nm, every 11 seconds. Then, using real-time spectral deconvolution analysis of the spectra, the concentrations of fluorescent phytoplankton pigments, including chlorophyll-*a*, were quantified from fluorescence normalized to water Raman scattering [2]. Data from the ship's thermosalinograph and GPS were fed into the ALFA unit and combined into a single data stream. Chlorophyll fluorescence from the ALFA was calibrated to extracted chlorophyll-*a* from discrete samples collected at different locations along the cruise track. For calibrations, water was filtered (0.2 µm polycarbonate filter) within an hour of collection, and filters were frozen (-20°C) until extraction in acetone or methanol. Extracted chlorophyll was quantified based on fluorescence using a Turner Designs fluorometer[1, 2].

Due to high variability in phytoplankton pigments associated with the Mississippi river plume, transects near GC600 with surface salinity lower than 35.6 were excluded from our analyses. Sections of the ship track within 3 km of GC600 were categorized as "seep" (S). The non-seep background statistics were calculated from portions of the same ship track segment that were > 3 km from GC600 and matched the salinity criteria.

Satellite imaging: A database of 176 SAR images that had been processed to identify surface oil-slick features in the Northern Gulf of Mexico was gridded into 10 x10 km cells as described by MacDonald *et al*[3, 4]. This database was used to identify the single grid cell with the highest cumulative area covered by slicks from 1997 to 2007. This site (centered at 27.15°N, 91.35°W) was designated "Alpha". In addition, four 50 x 50 km boxes with no incidence of oil slicks during the study period, located at a similar latitude as Alpha, and not routinely affected by the Mississippi river plume, were identified as non-seep background sites (Fig. 3A). Satellite-derived chlorophyll concentration time series for five 50 x 50 km boxes centered on Alpha and the four background sites were constructed using NASA Sea-viewing Wide Field-of-view Sensor (SeaWiFS) Level 3, 8-day composite, 9-km resolution chlorophyll data (NASA Ocean Biology

(OB.DAAC). Sea-viewing Wide Field-of-view Sensor (SeaWiFS) Ocean Color Data, 2014.0 Reprocessing. NASA OB.DAAC, Greenbelt, MD, USA. doi: 10.5067/ORBVIEW-2/SEAWIFS_OC.2014.0), averaging across pixels within each box. The size of this region of interest for chlorophyll observation was chosen to reflect how far currents might spread a surface oil slick in 8 days. The change in 8-day chlorophyll concentration in the 50 × 50 km area around site Alpha from one 8-day interval to the next ($\Delta[chl_8]$) could be estimated for 23 time intervals when an oil slick was observed directly at site Alpha. Excluding these slick events, $\Delta[chl_8]$ could also be calculated for Alpha over another 392 time intervals during the study period. For each of these time windows, $\Delta[chl_8]$ was also calculated at each of the four background sites, then averaged together to represent a mean background condition for comparison to Alpha. Thus, data from Alpha and the background sites represent the change in chlorophyll at each site across the same two 8-day time intervals, rather than the absolute chlorophyll concentrations, and comparisons between Alpha and the mean background were paired in time for analysis. The potential for the slicks to interfere with the optical measurements used for satellite-derived chlorophyll concentration was minimized because the slicks were identified in one 8-day time interval, while the chlorophyll response was measured from that interval to the next. Meanwhile, slick dissipation is usually rapid by comparison – MacDonald et al[5] calculated the half-life of a slick to range from 0.25 to maximum of 8 days.

References

1. Knap A, A. Michaels, A. Close, H. Ducklow, A. Dickson. 1996. Protocols for the Joint Global Ocean Flux Study (JGOFS) Core Measurements: JGOFS Report Nr. 19, vi+170 pp: Reprint of the IOC Manuals and Guides No. 29, UNESCO 1994.:

2. Chekalyuk A, Barnard A, Quigg A, Hafez M, Zhao Y. Aquatic laser fluorescence analyzer: field evaluation in the northern Gulf of Mexico. *Optics Express* 2014, **22**(18)**:** 21641-21656.

3. MacDonald IR, Garcia-Pineda O, Beet A, Asl SD, Feng L, Graettinger G, *et al.* Natural and Unnatural Oil Slicks in the Gulf of Mexico. *J Geophys Res* In press.

4. MacDonald IR, et al. . Neural network analysis determination of oil slick distribution and thickness from satellite Synthetic Aperture Radar, April 24 - August 3, 2010. (2015), Distributed by Gulf of Mexico Research Initiative Information and Data Cooperative (GRIIDC), Harte Research Institute, Texas A&M University – Corpus Christi DOI: 10.7266/N7KW5CZN.

5. Macdonald IR, Guinasso NL, Ackleson SG, Amos JF, Duckworth R, Sassen R, *et al.* Natural oil-slicks in the gulf-of-mexico visible from space. *J Geophys Res* 1993, **98**(C9)**:** 16351-16364.

Elevated surface chlorophyll associated with natural oil seeps in the Gulf of Mexico.

D'souza N.A.[1,3]; Subramaniam A.[1]; Juhl A.R.[1]; Hafez M.[1]; Chekalyuk A.[1]; Phan S.[1]; Yan B.[1]; MacDonald I.R.[2]; Weber S.C.[3]; Montoya J.P.[3]

[1] Lamont-Doherty Earth Observatory of Columbia University, Palisades, NY

[2] Florida State University, Tallahassee, Florida

[3] Georgia Institute of Technology, Atlanta, Georgia.

Supplementary Figures and Tables:

Supplementary Table 1: Dates and locations of CTD casts. Data from these CTD casts were used in Fig. 1.

Supplementary Table 2: Summary statistics for water column nutrient concentrations at GC600 and non-seep sites. Mean concentrations of NO_2^-+ NO_3^-, PO_4^{3-}, and SiO_2 for seep and non-seep sites were compared within depth bins using t-tests, n is the number of casts with data within a given depth bin. Statistical significance of NO_2^- + NO_3^- concentrations in the upper 3 depth bins were not tested because the values were below the detection limit. PO_4^{3-} data in the 106-157 m depth bin failed normality tests and was not analyzed by t-test, though the seep concentrations were significantly higher than the non-seep values using a Wilcoxon Rank-Sum test ($P < 0.001$). The 52-80 m and 158-202 m bins lacked sufficient observations to test statistical significance.

Supplementary Table 3: Summary statistics of near-surface chlorophyll concentrations near GC600 on three separate cruises. Summary statistics for the data shown in Fig. 2.

Supplementary Figure 1: Average water temperature profiles for seep and non-seep sites to 1200 m. Data are means ±1 s.e.m for 1-m depth bins.

Supplementary Table 1

	Date	Latitude	Longitude
Seep Sites	5/28/2012	27.36253	-90.5639
	5/28/2012	27.3628	-90.563
	5/28/2012	27.36117	-90.5752
	6/27/2012	27.3646	-90.5779
	6/27/2012	27.36107	-90.567
	6/28/2012	27.36092	-90.5789
	6/28/2012	27.36353	-90.564
	6/29/2012	27.36672	-90.5625
	6/29/2012	27.367	-90.56
Non-seep sites	5/29/2012	26.02533	-92.2523
	6/5/2012	27.81852	-89.0683
	6/5/2012	27.81738	-89.0629
	6/5/2012	27.81512	-89.0622
	6/9/2012	27.73773	-88.8381
	6/9/2012	27.72155	-88.317
	6/9/2012	27.67295	-88.7774
	6/9/2012	27.5802	-88.7215
	6/17/2012	27.92133	-86.6916
	6/30/2012	27.53693	-89.7668

Supplementary Table 2

Depth bin	NO_2+NO_3 (µM) Seep	Non-Seep	Stat Sig	p-value	PO_4 (µM) Seep	Non-Seep	Stat Sig	p-value	SiO_4 (µM) Seep	Non-Seep	Stat Sig	p-value
Depth 0-9	0 n = 6	0.055 n = 7	NA	NA	0.119 n = 6	0.102 n = 7	N	0.133 (t-test)	1.117 n = 6	0.816 n = 7	N	0.073 (t-test)
Depth 10-25	0.0021 n = 6	0 n = 6	NA	NA	0.119 n = 6	0.0913 n = 6	N	0.059 (t-test)	1.103 n = 6	0.964 n = 6	N	0.256 (t-test)
Depth 26-51	0 n = 8	0 n = 6	NA	NA	0.109 n = 8	0.0987 n = 6	N	0.303 (t-test)	1.131 n = 8	0.879 n = 6	Y	<0.001 (t-test)
Depth 52-80	0 n = 2	0.5043 n = 6	NA	NA	0.114 n = 2	0.112 n = 6	NA	NA	1.27 n = 2	1.244 n = 6	NA	NA
Depth 81-105	2.654 n = 6	0.528 n = 5	Y	<0.001 (t-test)	0.183 n = 6	0.121 n = 5	Y	0.002 (t-test)	2.071 n = 6	1.265 n = 5	Y	<0.001 (t-test)
Depth 106-157	12.379 n = 6	6.454 n = 5	Y	<0.001 (t-test)	0.713 n = 6	0.380 n = 5	NA	NA	4.827 n = 6	2.436 n = 5	Y	<0.001 (t-test)
Depth 158-202	17.932 n = 2	12.588 n = 4	NA	NA	1.254 n = 2	0.909 n = 4	NA	NA	8.666 n = 2	5.403 n = 4	NA	NA

Supplementary Table 3

Site – Date of sampling	GC600 - June 2012		GC600 - Sept 2012		GC600 - June 2013	
	B	S	B	S	B	S
Sample size (n)	190	1665	179	1250	154	3759
Mean ($mg.m^{-3}$)	0.0658	0.0629	0.0303	0.0397	0.0429	0.147
% increase in Mean		-4.41		31.02		242.66
Std. Dev. ($mg.m^{-3}$)	0.0147	0.0188	0.0075	0.0241	0.0070	0.0108
Variance	0.0002	0.0004	0.0001	0.0006	0.0001	0.0001
Median ($mg.m^{-3}$)	0.0628	0.0606	0.0300	0.0370	0.0414	0.1460
% increase in Median		-3.50		23.33		252.66
Min. ($mg.m^{-3}$)	0.0483	0.0334	0.0173	0.0186	0.0320	0.1240
Max. ($mg.m^{-3}$)	0.2200	0.3900	0.0694	0.7040	0.0744	0.2820
% increase in max.		77.27		914.41		279.03
Skewness	6.662	6.488	1.381	18.526	2.002	2.248
Kurtosis	64.407	91.145	4.442	476.413	5.928	16.557
P-value (when compared with B)		P <0.001		P <0.001		P <0.001

B = background
S = seep

Supplementary Figure 1